

# A statistical thermodynamic approach to sonochemical reactions

Bernard David<sup>a,\*</sup>, Primius Boldo<sup>b</sup>

<sup>a</sup> *Université de Savoie, ESIGEC, LCME, 73 376 Le Bourget du Lac, Cedex, France*

<sup>b</sup> *Université de Savoie, 73 376 Le Bourget du Lac, Cedex, France*

Received 12 December 2005; received in revised form 6 February 2007; accepted 8 February 2007

Available online 23 February 2007

## Abstract

The calculation of the equilibrium constants  $K$  of the sonolysis reactions of  $\text{CO}_2$  into  $\text{CO}$  and  $\text{O}$  atom, the recombination of  $\text{O}$  atoms into  $\text{O}_2$  and the formation of  $\text{H}_2\text{O}$  starting with  $\text{H}$  and  $\text{O}$  atoms, has been studied by means of statistical thermodynamic. The constants have been calculated at 300 kHz versus the pressure and the temperature according to the extreme conditions expected in a cavitation bubble, e.g. in the range from ambient temperature to 15200 K and from ambient pressure to 300 bar. The decomposition of  $\text{CO}_2$  appears to be thermodynamically favored at 15200 K and 1 bar with a constant  $K_1 = 1.52 \times 10^6$ , whereas the formation of  $\text{O}_2$  is not expected to occur ( $K_2 = 1.8 \times 10^{-8}$  maximum value at 15200 K and 300 bar) in comparison to the formation of water ( $K_3 = 3.4 \times 10^{47}$  at 298 K and 300 bar). The most thermodynamic favorable location of each reactions is then proposed, the surrounding shell region for the thermic decomposition of  $\text{CO}_2$  and the wall of the cavitation bubble for the formation of water.

Starting from a work of Henglein on the sonolysis of  $\text{CO}_2$  in water at 300 kHz, the experimental amount of  $\text{CO}$  formed ( $7.2 \times 10^{20}$  molecules  $\text{L}^{-1}$ ) is compared to the theoretical  $\text{CO}$  amount ( $1.4 \times 10^{27}$  molecules  $\text{L}^{-1}$ ) which can be produced by the sonolysis of the same starting amount  $\text{CO}_2$ . With the help of the literature data, the number of cavitation bubble has been evaluated to  $6.2 \times 10^{15}$  bubbles  $\text{L}^{-1}$  at 300 kHz, in 15 min. This means that about 1 bubble on 1900000 is efficient for undergoing the sonolysis of  $\text{CO}_2$ .

© 2007 Elsevier B.V. All rights reserved.

**Keywords:** Statistical thermodynamic; Carbon dioxide sonolysis; Equilibrium constant; Temperature; Pressure

## 1. Introduction

Acoustic cavitation in aqueous solution gives rise to the formation of micrometer bubbles. These bubbles grow and implode when they reach a critical size. The collapse of the cavitation bubble is extremely rapid in few hundred picoseconds, and the heating and cooling is greater than  $10^9 \text{ K s}^{-1}$  [1]. As a result of the implosion, high energy phenomena are generated in the medium such as the cleavage of chemical bonds when chemistry is involved, erosion and emission of light from excited species for mechanical and photophysical effects, respectively. Experimental works from Suslick have first shown that when solutions of metal

carbonyls, used as spectroscopic probe, are irradiated at 20 kHz under Argon in a silicone oil and in presence of a multi bubble system, the temperature ( $T$ ) inside the bubble of cavitation grows up to  $4700 \pm 300 \text{ K}$  [2]. Recently, evidence for higher temperature up to  $15200 \pm 1900 \text{ K}$  lightened the possibility of a highly ionized plasma core, in regard to a single bubble system obtained at 20 kHz in aqueous  $\text{H}_2\text{SO}_4$  solution under Ar, with an acoustic pressure ranging from 1.3 to 6 bar [3]. In addition, calculations in water at 52 kHz showed that the maximum temperature could increased up to 6500 K in a single air bubble system whereas the maximum would be 10900 K in a single Ar bubble system, with an acoustic pressure range of 1.3–1.5 bar [4]. A theoretical temperature value at 300 kHz is given in water by Hoffmann, i.e. 6920 K with  $P_a = 2 \text{ bar}$  [5]. In this last paper, it is alleged that the temperature can rise up to 14700 K in case of drier mixture but

\* Corresponding author. Tel.: +33 (0) 4 79 75 88 03; fax: +33 (0) 4 79 75 88 85.

E-mail address: [bernard.david@univ-savoie.fr](mailto:bernard.david@univ-savoie.fr) (B. David).

## Nomenclature

$a$	Van der Waals coefficient ( $L^2 \text{ bar mol}^{-2}$ )	$P_v$	water vapor pressure within the bubble (bar)
$b$	Van der Waals coefficient ( $L \text{ mol}^{-1}$ )	$r$	bubble radius ( $\mu\text{m}$ )
$\Delta U^\circ$	internal energy of the reaction at 0 K ( $\text{J mol}^{-1}$ )	$R$	constant of perfect gases $8.31 \text{ J mol}^{-1} \text{ K}^{-1}$
$\eta$	shear viscosity of water ( $\text{mPa s}$ )	$R_0$	equilibrium radius of a spherical bubble ( $\mu\text{m}$ )
$f$	frequency of the wave (kHz)	$\rho$	density of water ( $\text{kg m}^{-3}$ )
$g_{\text{vib.}}$	vibrational degeneration	$\sigma$	symmetry factor
$g_{\text{elec.}}$	electronic degeneration	$\sigma_w$	water surface tension ( $\text{N m}^{-1}$ )
$\gamma$	polytropic ratio, $\gamma = C_p/C_v$	$T$	temperature (K)
$h$	Planck constant (J s)	$T_a$	ambient temperature (K)
$I$	inertia moment towards a rotational motion ( $\text{kg m}^2$ )	$\theta$	characteristic temperature (K)
$k$	Boltzmann constant ( $\text{J K}^{-1}$ )	$\theta_{\text{vib.}}$	characteristic temperature of vibrational motions (K)
$\kappa$	polytropic index of argon	$\theta_{\text{elec.}}$	characteristic temperature from electronic transitions (K)
$m$	molecular weight ( $\text{kg molecule}^{-1}$ )	$\theta_x$	characteristic temperature on ( $O_x$ ) axe, associated to the inertia moment $I_x$ , (K)
$M$	$\text{mol L}^{-1}$	$\theta_y$	characteristic temperature on ( $O_y$ ) axe, associated to the inertia moment $I_y$ , (K)
$n$	mole number (mol)	$\theta_z$	characteristic temperature on ( $O_z$ ) axe, associated to the inertia moment $I_z$ , (K)
$N$	molecule number (molecule)	$V$	volume of a cavitation bubble ( $\text{m}^3$ )
$N$	bubble number for 1 L of sonicated solution	$v$	volume ( $\text{m}^3$ )
$\mathcal{N}$	Avogadro constant ( $\text{mol}^{-1}$ )	$Z$	the total partition function which can expressed as: $Z = Z_{\text{translation}} \cdot Z_{\text{rotation}} \cdot Z_{\text{vibration}} \cdot Z_{\text{electronic}} \cdot Z_{\text{nuclear}}$
$v_i$	the stœchiometric coefficient (products: $v_i > 0$ and reactants: $v_i < 0$ )		
$P$	pressure (bar)		
$P_a$	acoustic pressure (bar)		
$P_{\text{gas}}$	gas pressure in the bubble at the initiation of the collapse (bar)		
$P_0$	atmospheric pressure (bar)		
$P_{\text{hyd.}}$	hydrostatic liquid pressure outside the bubble (Pa)		

conclude that as bubbles involved in sonochemistry are largely filled with water vapor, their temperature will be around 10000 K due to chemical reactions. Recent works also showed that the temperature at 355 kHz in water could be 4600 K [6,7].

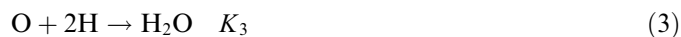
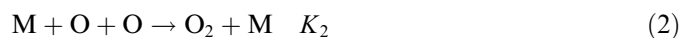
On the other hand, the experimental pressure ( $P$ ) measured reaches about  $300 \pm 30$  bar in argon-saturated silicone oil with a multi bubble system at 20 kHz [8]. Theoretical data at low frequency on the evolution of the intracavity pressure is also available in the literature, from the birth to the collapse of cavitation bubble [9–11]. Extreme limit predicted for  $P$  is 1000 bar in association with a maximum temperature 10000 K. Both thermodynamic  $T$  and  $P$  values, fit quite well with the hypothesis of an adiabatic compression of the bubble during the cavitation collapse.

Using ultrasounds as an advanced oxidative technology, it appears that a large range of sonochemical degradation reactions of hydrophobic pollutants present in water, or adsorbed on mineral supports in aqueous suspensions, lead to the formation of gases like  $\text{CO}_2$  and CO [12–15]. The combustion and/or the pyrolysis of the hydrophobic pollutants are often expected to occur inside or near the bubble of cavitation. Both compounds,  $\text{CO}_2$  and CO, are good

indicators of the mineralization yield of the starting material during the process. The presence of CO in the sonochemical degradation of organic compounds is often assumed to be due to a deficit of oxygen in the medium with an incomplete combustion of the substrate. Nevertheless, as mentioned by Henglein [16], CO can also be formed from the decomposition of  $\text{CO}_2$  within the bubble of cavitation, according to the following reaction, where M is the third body [4,17]:



The oxygen atoms can lead to  $\text{O}_2$  and  $\text{H}_2\text{O}$  [8,13,14]:



where H atoms arise from the sonolysis of water:



According to the reaction (2), dioxygen would be generated, limiting therefore the oxygen deficit in the cavitation bubble. These reactions have been postulated by Henglein to occur in the bubble of cavitation at high frequency 300 kHz. However, no examination of the thermodynamic

conditions have been done for these reactions. In this work, we mainly focused our attention on the thermodynamic conditions which favor the ultrasonic conversion of  $\text{CO}_2$  by developing the expression of the equilibrium constant  $K_1$  versus  $T$  and  $P$  at 300 kHz. The equilibrium constants  $K_2$  and  $K_3$  are also determined in order to predict the behavior of oxygen atoms in the bubble towards reactions (2) and (3). It is then proposed to examine the area where the reactions take place towards the cavitation bubble.

Assuming that bubbles of cavitation are microreactors which adiabatically collapse [18], it seems useful to apply the statistical thermodynamic at the molecular level, contrary to the classic macroscopic thermodynamic who is working at global scale. Every thermodynamic property of a system is encoded in its partition function  $Z$ , a sum which runs over all possible states that the system can assume, at specific temperature and pressure. The partition function  $Z$  introduced in statistical thermodynamic represents the bridge between the *ab initio* and the thermodynamic scales. Both approaches do not be opposed since they are often mutually dependent (Annex 1). In addition, it is also possible to find in the literature interesting databases including *ab initio* calculations, especially in the combustion field, which allow the determination of thermodynamic data (CANTERA for equilibrium constant of reactions as example of chemical – see Annex 1). Nevertheless, the limitation of these databases is mainly on the presently highest temperature value around 3000–4000 K. The high temperature limit can be exceeded with the help of statistical thermodynamic by assuming that spectroscopic data are constant in the extreme temperature range. Starting with the highest experimental limits presently known for  $T$  and  $P$  in the literature, we chose to elaborate calculations from ambient conditions to these extreme conditions [3,8].

In a second part of this study, a particular attention concerned an hypothesis postulated by Henglein on the sonolysis of carbon dioxide in aqueous solution [16]. It is assumed that gas bubbles are not in Henry's equilibrium with the surrounding aqueous gas solution. Indeed, the maximum in the CO yield during the sonolysis of  $\text{CO}_2$  under an Ar atmosphere, appears at very low concentration of  $\text{CO}_2$  in water (molar fraction  $x_{\text{CO}_2} = 0.01$ ). It is then concluded that the mole fraction of  $\text{CO}_2$  in the gas bubbles is much larger than in the gas atmosphere under which the ultrasonic irradiation is carried out. So we examined at the microscopic level, the possibility of a fast  $\text{CO}_2$  gas pumping from the solution within the bubbles of cavitation.

## 2. Thermodynamic conditions of the cavitation

First works on the cavitation phenomenon assumed that the compression phase of the bubbles of cavitation is an adiabatic one [18–20]. An adiabatic process is one in which no heat is gained or lost by the system, here the bubble of cavitation. All the change in internal energy is in the form of work or heat done, as provided for the first law of ther-

modynamic. Versus different parameters, it is then possible to predict the evolution of temperature and pressure occurring in a bubble of cavitation, according to the following equations [19]:

$$T = \frac{T_a \cdot P_a \cdot (\gamma - 1)}{P_{\text{gas}}} \quad (5)$$

$$T_f = T_i \cdot (r_i/r_f)^{3(\gamma-1)} \quad (6)$$

$$P_f = P_i \cdot (r_i/r_f)^{3\gamma} \quad (7)$$

where i and f refer to initial and final conditions of the temperature  $T$ , pressure  $P$  and radius  $r$ .

The main conclusion of relation (5) is that an increase of the gas pressure inside the bubble of cavitation enhances the decrease of the temperature reached during the collapse. Nevertheless, previous equations neglect solvent or the vapor pressure of chemical compounds and especially chemical reactions.

What it is presently known on the thermodynamic of the cavitation bubble in water, is that the initial temperature and pressure in the bulk (water) are near from ambient for  $T$ , and near from the acoustical pressure  $P_a$  added to the ambient pressure  $P_0$  for  $P$ . In this work the final values chosen for  $T$  and  $P$  at the end of the collapse are the following extreme experimental data: 15200 K and 300 bar. It seems important in our calculations, to do not exclude the possibility of very high temperature in water. According to the introduction of some new parameters (such as  $P_v$ ,  $\sigma_w$ ,  $\eta$ , etc.) in the statistical thermodynamic model, it would also be possible to get data for reactions occurring in solvent other than pure water (water in presence of  $\text{H}_2\text{SO}_4$ , as example).

In order to predict the equilibrium constant during a sonochemical reaction, it is important to control the

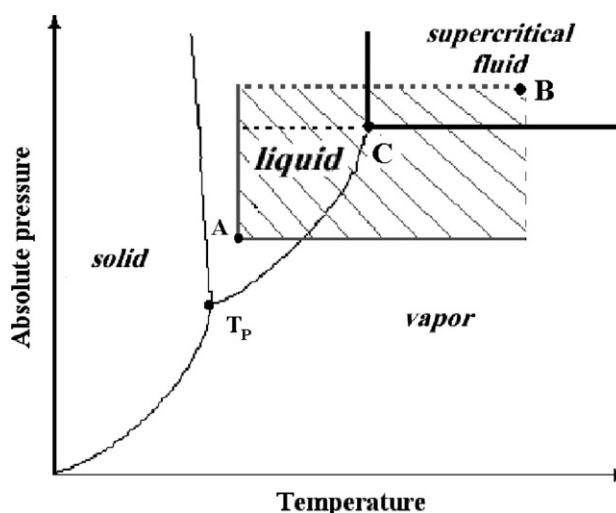


Fig. 1. Phase diagram of water superposed to the hashed zone corresponding to the extreme variations of pressure and temperature occurring in a cavitation bubble.  $T_p$  = triple point (273 K, 0.006 bar); A = initial conditions from the bulk (298 K, 1 bar); C = critical point (647 K, 200 bar); B = extreme final conditions at the collapse of the bubble of cavitation (15200 K, 300 bar).

evolution of the temperature and pressure from the bulk solution to the collapse of the bubble of cavitation. Fig. 1 shows the phase diagram of water with a hashed zone corresponding to the possible thermodynamic conditions occurring in a cavitation bubble including the supercritical zone.

A great number of reactions occurring in the cavitation bubble takes place in the supercritical phase where water behaves as well as a liquid and a gas. But up to now, if the right way from A to B is an adiabatic transformation, the recent discovery of plasma inside the bubble may disturb this way. This is why we chose to investigate calculations of equilibrium constants in the hashed zone where temperature and pressure can vary independently. A scanning of temperature is undertaken from 298 to 15200 K and from 1 to 300 bar for pressure. In these conditions, it is expected that the gas present inside the bubble of cavitation is more correctly described by using the Van der Waals equation for real gases which behave differently from the perfect gases especially at high pressure and low temperature,

$$P = \frac{nRT}{V - nb} - a \cdot \left(\frac{n}{V}\right)^2 \quad (8)$$

with  $a$  and  $b$  the Van der Waals coefficients.

### 3. Treatment of sonochemical reactions from a statistical point of view

It is possible to calculate the equilibrium constants  $K$  for reactions (1)–(3) by using the statistical thermodynamic, where  $K$  is expressed according to the following expression [21–23]:

$$K = \prod_i \left(\frac{Z}{N}\right)^{v_i} \cdot \exp(-\Delta U^\circ/RT) \quad (9)$$

where  $i$  refers to the reactants and products of the reaction studied. The partition function  $Z$  is a key function in statistical thermodynamic which represents the different microstate energies corresponding to translation, rotation, vibration motions and to the electronic states of molecules. It can be noticed that there is no nuclear contribution ( $Z_{\text{nuclear}}$ ) to the total partition function  $Z$  and then to the equilibrium constant, because  $\prod_i (Z_{\text{nuclear}})^{v_i} = 1$ . The equilibrium constant  $K$  can be written:

$$K = \prod_i \left(\frac{Z_{\text{translation}} \cdot Z_{\text{rotation}} \cdot Z_{\text{vibration}} \cdot Z_{\text{electronic}}}{N}\right)^{v_i} \cdot \exp(-\Delta U^\circ/RT)$$

The individual  $Z$  partition functions detailed in Table 1 are calculated with the help of spectroscopic terms which are then expressed in term of characteristic temperature  $\theta$  in Table 2.

Taking into account all these parameters, the equilibrium constants  $K$  of the previous reactions can be expressed versus the temperature and pressure. By using the equation

Table 1

Mathematical expressions of the different partition functions  $Z$  and the corresponding characteristic temperatures  $\theta$

Energy type	Partition function	$\theta$ (K)
Translation	$Z = (2mkT\pi)^{3/2} \cdot \frac{V}{h^3}$	Not used
Rotation, diatomic molecule	$Z = \left(\frac{T}{\sigma \cdot \theta_{\text{rot}}}\right)$	$\theta_{\text{rot}} = \frac{h^2}{8\pi^2 \cdot I \cdot k}$
Rotation, polyatomic molecule	$Z = \left(\frac{\sqrt{\pi} T^{3/2}}{\sigma \cdot \sqrt{\theta_x \theta_y \theta_z}}\right)$	$\theta_x = \frac{h^2}{8\pi^2 \cdot I_x \cdot k}$ $\theta_y = \frac{h^2}{8\pi^2 \cdot I_y \cdot k}$ $\theta_z = \frac{h^2}{8\pi^2 \cdot I_z \cdot k}$
Vibration	$Z = \prod_i \frac{1}{(1 - \exp(-\theta_{\text{vib},i}/T))^{\nu_{\text{vib},i}}}$	$\theta_{\text{vib},i} = \frac{h \cdot \nu_{\text{vib},i}}{k}$
Electronic	$Z = \sum_i g_{\text{elec},i} \cdot \exp(-\theta_{\text{elec},i}/T)$	$\theta_{\text{elec},i} = \frac{h \cdot \nu_{\text{elec},i}}{k}$

of Van der Waals, it involves that in the expression of  $Z_{\text{translation}}$ ,  $V$  is expressed versus  $T$ ,  $P$ ,  $a$ ,  $b$  ( $a$  and  $b$  values in Table 2). It is then necessary to resolve a cubic equation giving two complex solutions and only one real solution which can be expressed by the Cardan's formula [24]. The calculation of the different equilibrium constants expressions on SigmaPlot® are made with a  $T$  range:  $T_{\text{min}} = 298$  to  $T_{\text{max}} = 17000$  K with a  $T_{\text{increment}} = 500$  K, and with a  $P$  range:  $P_{\text{min}} = 1$  to  $P_{\text{max}} = 350$  bar, with a  $P_{\text{increment}} = 50$  bar.

#### 3.1. Sonolysis of CO<sub>2</sub>

The final mathematical expression of the equilibrium constant  $K_1$  for the sonolysis of CO<sub>2</sub> (1) appears below as a programming line on SigmaPlot®:

$$\begin{aligned} K_1(\text{CO}_2) = & (4.21 * 10^3) * T^{1.5} * V \\ & * (5 + 3 * \exp(-225/T) + \exp(-325/T)) \\ & * ((1 - \exp(-960/T))^{1/2}) \\ & * (1 - \exp(-1820/T)) * (1 - \exp(-3280/T)) \\ & * \exp(-3.381 * 10^4/T) \\ & / (1 - \exp(-3085/T)) \end{aligned}$$

where the internal energy  $\Delta U^\circ$  (0 K) from reaction (1) is 281 kJ mol<sup>-1</sup>, estimated from the enthalpy of formation of each compound [25,26].

The volume  $V$  is expressed versus  $T$  and  $P$  according to the following equations from Cardan:

$$\begin{aligned} a &= 0.3640 \\ b &= 4.267 * 10^{-5} \\ a1 &= -(b + 8.31 * T / (P * 10^5)) \\ a2 &= a / (P * 10^5) \\ a3 &= -a * b \\ p &= a2 - a1^{2/3} \\ q &= 2 * a1^{3/27} - a1 * a2 / 3 + a3 \\ P &= (-q/2 + \text{sqrt}(p^3/27 + q^2/4))^{1/3} \\ Q &= (-q/2 - \text{sqrt}(p^3/27 + q^2/4))^{1/3} \\ V &= P + Q - a1/3 \end{aligned}$$

The  $a$  and  $b$  values from CO<sub>2</sub> are assumed to remain constant during the reaction.

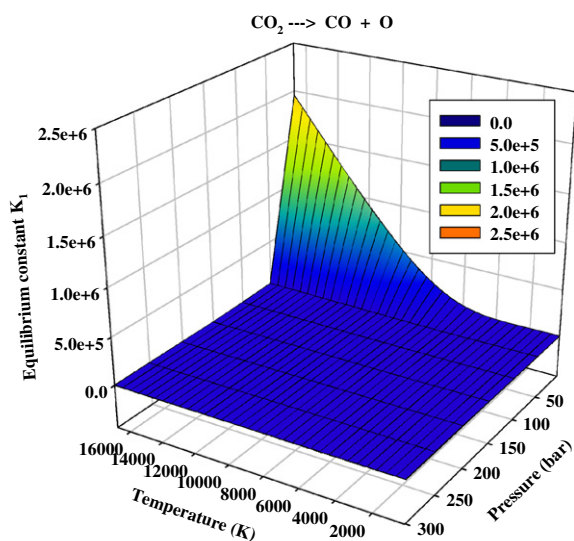
Table 2

Data available for the calculation of the different partition functions  $Z$  and the equilibrium constants  $K$  for the reactions studied [22,23,26]

	$\theta_{\text{vib.}}$ (K), degeneration $g_{\text{vib.}}$	$\theta_{\text{rot.}}^{\text{a}}$ (K) or $\theta_x, \theta_y, \theta_{\text{zrot.}}^{\text{b}}$ (K)	$\theta_{\text{elec.}}^{\text{c}}$ (K)	$\sigma$	Van der Waals coefficient	
					$a$ ( $\text{L}^2 \text{ bar mol}^{-2}$ )	$b$ ( $\text{L mol}^{-1}$ )
H	–	–	0 ( $g = 1$ ) 118260 ( $g = 4$ )	–	–	–
O	–	–	0 ( $g = 5$ ) 225 ( $g = 3$ ) 325 ( $g = 1$ ) 22700 ( $g = 5$ )	–	–	–
O <sub>2</sub>	2773 ( $g = 1$ )	2.10	0 ( $g = 3$ ) 11300 ( $g = 2$ ) 18500 ( $g = 1$ )	1	1.360	0.03183
CO	3085 ( $g = 1$ )	2.60	0 ( $g = 1$ ) 93643 ( $g = 1$ )	1	1.485	0.03985
CO <sub>2</sub>	960 ( $g = 2$ ) 1820 ( $g = 1$ ) 3280 ( $g = 1$ )	0.54	0 ( $g = 1$ ) 66194 ( $g = 1$ )	2	3.640	0.04267
H <sub>2</sub> O	2690 ( $g = 3$ )	40.38, 21.08, 13.49	0 ( $g = 1$ ) 2290 ( $g = 1$ ) 5370 ( $g = 1$ ) 5510 ( $g = 1$ )	2	5.460	0.03050

<sup>a</sup> Diatomic molecule.<sup>b</sup> Polyatomic molecule.<sup>c</sup> The origin of electronic energies is made on the fundamental electronic state.

In Fig. 2, the equilibrium constant  $K_1$  appears to be 300-fold higher at low pressure (1 bar) and at high temperature (15200 K) than at high temperature and pressure (15200 K, 300 bar) with  $K_1 = 1.5 \times 10^6$  and  $4.7 \times 10^3$ , respectively. As shown in Fig. 3a and b,  $K_1$  values are high whatever the pressure at very high temperature 15200 K, whereas  $K_1$  is null at low temperature ( $T < 4000$  K) and 1 bar. Therefore with these high  $K_1$  values calculated at high temperature, the reaction (1) is thermodynamically favored inside the bubble.

Fig. 2. Equilibrium constant  $K_1$  versus temperature and pressure.

The sonolysis of CO<sub>2</sub> will be optimum if the reaction occurs in the first shell of the bubble where the temperature grows up but not the pressure rather than in the hot heart of the bubble of cavitation (300 bar and 15200 K). As shown by Henglein, the formation of CO is the main product arising from the sonolysis of CO<sub>2</sub>, proving that the reaction occurs from a thermodynamic and a kinetic point of view.

### 3.2. Formation of O<sub>2</sub> under ultrasound

As predicted by the statistical thermodynamic, the equation for the calculation of  $K_2$  is:

$$K_2(\text{O}_2) = (1 * 10^{-4}) * \exp(-58464 / T) / ((1 - \exp(-2773 / T)) * (5 + 3 * \exp(-225 / T) + \exp(-325 / T))^2 * V * x^{1/2})$$

with  $V$  which has been calculated in the same way than for CO<sub>2</sub>, using O<sub>2</sub> data for the Van der Waals coefficients in the lack of data for O atom. The internal energy  $\Delta U^\circ$  (0 K) from reaction (2) is estimated to  $-58.5 \text{ kJ mol}^{-1}$  [25,26].

As it is shown in Fig. 4, the reaction (2) of O<sub>2</sub> formation is favored for the high temperature and the high pressure. In this case this is the heart of the cavitation bubble which is involved. Nevertheless the absolute value of  $K_2$  is very low, about  $1.9 \times 10^{-8}$  at 15200 K and 300 bar and does not favor the formation of O<sub>2</sub> by recombination of O atoms rather than the dissociation of O<sub>2</sub>. Henglein showed that the reaction is kinetically possible but not

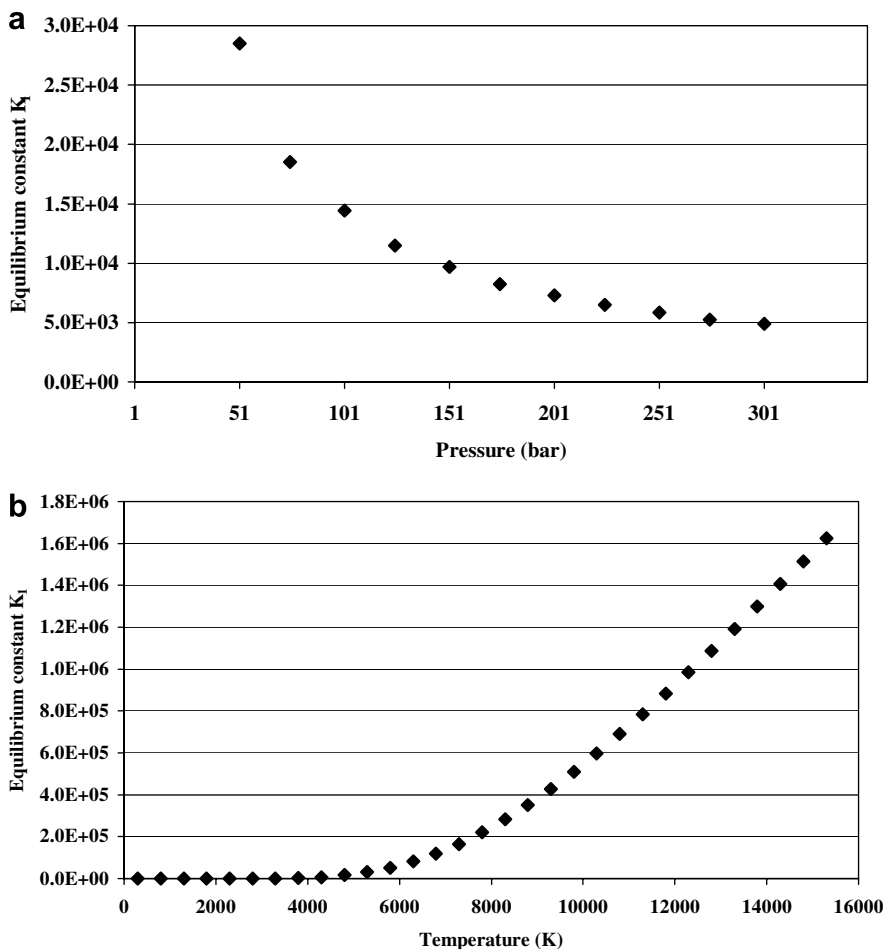


Fig. 3. (a) Profile of the evolution of  $K_1$  at 15200 K versus the pressure, ( $K_1 = 1.6 \times 10^6$  at 1 bar, does not appear on the figure); (b) profile of the evolution of  $K_1$  at 1 bar versus temperature.

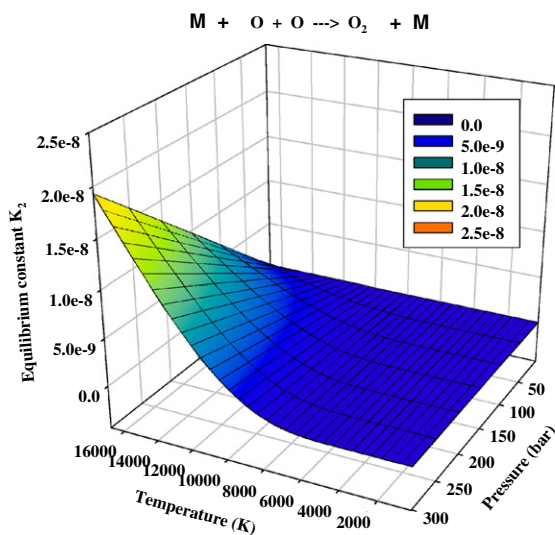


Fig. 4. Equilibrium constant  $K_2$  versus temperature and pressure.

predominant in the sonolysis of  $\text{CO}_2$ . The yield of  $\text{O}_2$  formation is about 25 times smaller than the CO yield. In addition, Yasui et al. found that  $\text{O}_2$  could mainly provide from another reaction:  $\text{O} + \text{OH} \cdot + \text{M} \rightarrow \text{O}_2 + \text{H} + \text{M}$  [4].

### 3.3. Formation of $\text{H}_2\text{O}$ under ultrasound

The expression of  $K_3$ , corresponding to the formation of  $\text{H}_2\text{O}$ , versus temperature and pressure is:

$$K_3(\text{H}_2\text{O}) = (1.21 \cdot 10^{-5}) \cdot (T^{\wedge} - 3) \cdot (V^{\wedge} - 2) \cdot (8.27 \cdot 10^{-3}) \cdot (x^{\wedge} 1.5) \cdot ((5 + 3 \cdot \exp(-225 / T) + \exp(-325 / T))^{\wedge} - 1) \cdot ((1 - \exp(-2690 / T))^{\wedge} - 3) \cdot (1 + \exp(-2290 / T) + \exp(-5370 / T) + \exp(-5510 / T)) \cdot \exp(34657 / T)$$

with  $a$  and  $b$  arising from  $\text{H}_2\text{O}$ , the final product of the reaction. The internal energy  $\Delta U^\circ$  (0 K) from reaction (3) is estimated to  $-288 \text{ kJ mol}^{-1}$  [25].

The very high value of  $K_3 = 3.4 \times 10^{47}$  at 298 K and 300 bar, suggests a complete shift of the equilibrium towards the formation of  $\text{H}_2\text{O}$  (Fig. 5). The reaction would be localized at the external of the bubble of cavitation where the temperature is near ambient. The shock wave generated by the collapse of the bubble could be then responsible of this reaction. Atoms would be ejected from

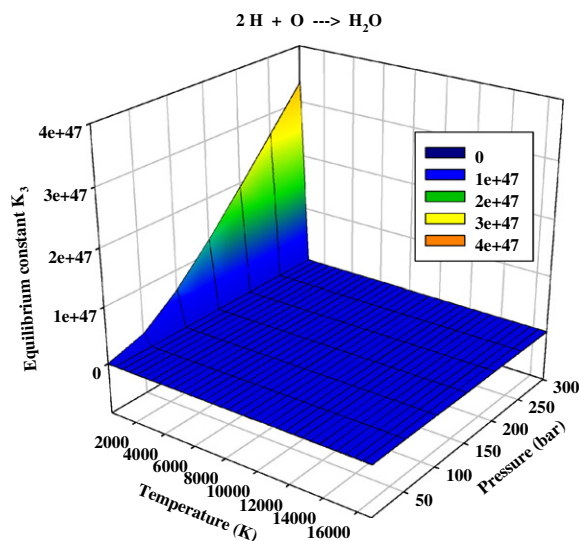


Fig. 5. Equilibrium constant  $K_3$  versus temperature and pressure.

the heart of the bubble to the surrounding shell, where they condense on the cold water wall from the bulk (see Fig. 6b).

The statistical thermodynamic provides informations on the equilibrium constants versus temperature and pressure, and allows to predict the  $T$  and  $P$  values which favor the reaction. Therefore the different thermodynamic areas of the reaction towards the bubble of cavitation can be predicted as described in Fig. 6a and b.

According to the thermal gradient within and close to the cavitation bubble, it is expected that light species are concentrated in the core of the bubble whereas higher molecular weight species are located in the surrounding shell [9,27]. This means that H, O,  $H_2O$ , CO,  $O_2$ , Ar and  $CO_2$  (listed by increasing molecular mass) are distributed from the hot core for H and O to the shell for Ar and  $CO_2$ . The decomposition of  $O_2$  (reverse reaction (1)) and of  $CO_2$  (reaction (2)) have been found to occur in the bubble core and in the vicinity of the core respectively, as expected on Fig. 6b. These two reactions are in a quite

good agreement with the thermal conductivity theory. The reaction (3) is located near the wall of the cavitation bubble in our model (Scheme 6b) and should appear at the interfacial area of the bubble according to the thermal theory.

An additional point is given in Annex 2, in order to underline differences which occur between the use of CANTERA database and the statistical thermodynamical data obtained.

#### 4. Estimation of an active bubble ratio under sonication

Starting from the well defined experimental results of Henglein on the aqueous sonolysis of  $CO_2$  under an Ar-atmosphere, the hypothesis concerning an increasing molar fraction of  $CO_2$  in the bubble of cavitation just before the collapse, has been studied. This means that bubbles could act as a pump for the dissolved gases just neighboring the bubble.

By knowing the amount of experimentally CO formed in the atmosphere of the reactor, it is possible to evaluate the real total amount of  $CO_2$  transformed at the interfacial area of the bubble. If we then compare the experimental CO formed with the amount of CO calculated by means of the previous equilibrium constant  $K_1$  (where the conditions are the most favorable, about 15200 K and 1 bar) three cases are possible:

- (i)  $[CO]_{\text{calculated}} \ll [CO]_{\text{experimental}}$ : the deficit in CO calculated could be due to a bad estimation of the number of  $CO_2$  molecules concerned by the reaction, in favor of a  $CO_2$  pumping motion in the bubbles.
- (ii)  $[CO]_{\text{calculated}} \approx [CO]_{\text{experimental}}$ : no need for pumping the dissolved gas around the bubble.
- (iii)  $[CO]_{\text{calculated}} \gg [CO]_{\text{experimental}}$ : overestimation of the number of cavitation occurrence, i.e. the number of efficient cavitation bubble is too high.

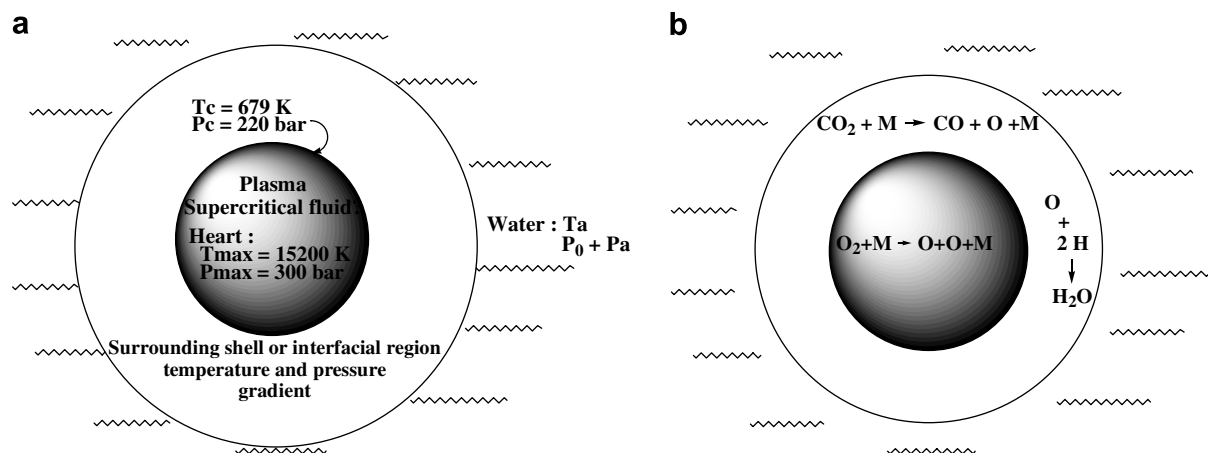


Fig. 6. (a) Scheme of the different thermodynamical conditions occurring within the bubble of cavitation; (b) location of the three concerned ultrasonic reactions.

#### 4.1. Theoretical amount of CO<sub>2</sub> inside the bubble

According to the Minneart and to the more simple Galli equations, the size of bubbles formed under an ultrasonic field is inversely proportional to the frequency of the wave [28,29]. Nevertheless, at acoustical pressures used in sonochemistry (3.2 bar in Henglein's work) the resolution of Rayleigh–Plesset has to be carried out [9,30–32]. The conditions of use of this equation are described in Annex 3. The equilibrium radius  $R_0$  calculated corresponds to the maximum authorized value of bubble radius which leads to a collapse. The resulting bubble diameter of a high frequency bubble at 300 kHz (Henglein conditions) is 62  $\mu\text{m}$ . In the lack of experimental result at 300 kHz in the literature, we chose to present calculations with this maximum theoretical value of bubble radius and not with a size distribution (1–62  $\mu\text{m}$ ). However, it can be noticed that experimental values measured are often lower than theoretical values, especially at 20 kHz [33,34].

The volume of the bubble and then the volume of gas inside such bubble is  $9.98 \times 10^{-10}$  L. When bubbles formed under the ultrasonic field are entirely filled with the Ar/CO<sub>2</sub> dissolved gas, with a partial pressure  $P_{\text{CO}_2} = 0.01$  bar at 298 K, the molecule number of CO<sub>2</sub> authorized inside one bubble is  $2.4 \times 10^{11}$  by using the Eq. (8). The Van der Waals coefficients are then those from Ar ( $a = 1.35 \text{ L}^2 \text{ bar mol}^{-2}$ ;  $b = 0.032 \text{ L mol}^{-1}$ ) the major gas inside the bubble.

On the other hand, it can be assumed that the composition of the atmosphere inside the bubble is the same that the dissolved gas just around the bubble, whatever the solubility of each gas in water ( $2 \times 10^{-3}$  M for Ar and  $3 \times 10^{-2}$  M for CO<sub>2</sub>). With the help of the Henry's law ( $K_{\text{H}(\text{CO}_2)} = 33.8 \times 10^{-3} \text{ mol L}^{-1} \text{ bar}^{-1}$ ), the concentration of CO<sub>2</sub> in water is then  $[\text{CO}_{2\text{aq.}}] = K_{\text{H}} \cdot P_{\text{CO}_2} = 33.8 \times 10^{-3} \times 0.01 = 33.8 \times 10^{-5} \text{ M}$ . The maximum number of carbon dioxide molecule in the gaseous atmosphere of one bubble would be then  $33.8 \times 10^{-5} \times 9.98 \times 10^{-10} \times \mathcal{N} = 2.03 \times 10^{11}$  molecules/bubble for a bubble radius of 62  $\mu\text{m}$ . This result is finally in good accordance with the molecule number inside the gaseous phase of one bubble with the previous Van der Waals equation.

The void fraction which can be defined as the bubble volume generated in a known volume of solution during one ultrasonic cycle has been measured at 308 kHz in aer-

ated water, with the help of a global hyperfrequency method [35,36]. This void fraction expressed as  $4\pi r^3 \cdot N / (3v)$  is useful in order to estimate the number  $N$  of bubble of cavitation generated in the medium. At 308 kHz, close to the frequency of Henglein's work 300 kHz, the void fraction is given to  $3 \times 10^{-4}$  with an acoustical pressure equal to 0.2 bar. With the hyperfrequency method used a linear relationship is theoretically expected and experimentally obtained between the void fraction and the acoustical pressure. Extrapolation of the void fraction at 3.2 bar (Henglein conditions) leads to a value of  $7.5 \times 10^{-3}$  [10,30,35,36]. The total number of sonolyzed CO<sub>2</sub> molecule within the supercritical/plasma phase of the bubble, during 15 min of irradiation time in 1 L, is then presented in Table 3. Results underline that the predicted CO<sub>2</sub> amount is extremely high and should correspond to an average aqueous CO<sub>2</sub> concentration of about  $[\text{CO}_{2\text{aq.}}] = 2 \times 10^3 \text{ M}$  and then to a partial pressure of CO<sub>2</sub> in the gas phase close  $P_{\text{CO}_2} = 65000 \text{ bar}$ , which has definitely never been measured.

#### 4.2. Experimental concentration of CO produced by the sonolysis of CO<sub>2</sub>

In Henglein's work, the CO concentration reaches  $11.7 \times 10^{-4} \text{ M}$  in the gas phase (i.e.  $7.04 \times 10^{20}$  molecules  $\text{L}^{-1}$ ). The CO partial pressure at 298 K is then  $P_{\text{CO}} = RT \times [\text{CO}_{(\text{g})}] = 8.31 \times 298 \times 11.7 \times 10^{-4} / 10^{-3} = 2.89 \times 10^3 \text{ Pa} = 2.9 \times 10^{-2} \text{ bar}$ . In addition, as CO is in equilibrium between the gas and the aqueous phase, the molecule number in solution can be evaluated with the Henry constant  $[\text{CO}_{(\text{aq.})}] = K_{\text{H}} \times P_{\text{CO}} = 0.98 \times 10^{-3} \times 2.9 \times 10^{-2} = 2.8 \times 10^{-5} \text{ M}$  (i.e.  $1.7 \times 10^{19}$  molecules  $\text{L}^{-1}$ ). The total CO molecule number is  $(7.04 \times 10^{20} + 1.7 \times 10^{19}) = 7.21 \times 10^{20}$  molecules  $\text{L}^{-1}$ . By using the  $K_1$  value at 15200 K and 300 bar and the predicted amount of CO<sub>2</sub> sonolyzed  $\approx 1.4 \times 10^{27}$  molecules  $\text{L}^{-1}$ , the theoretical CO molecule number is also estimated to  $\approx 1.4 \times 10^{27}$  molecules  $\text{L}^{-1}$ , far from the previous experimental value  $7.04 \times 10^{20}$  molecules  $\text{L}^{-1}$ .

In regard to the starting hypotheses, it can be concluded that the calculated concentration of CO formed is  $10^7$  time higher than the experimental one. That means that either the number of cavitation bubbles is overestimated or that

Table 3  
Estimation of the bubble number in 1 L per cycle and the number of CO<sub>2</sub> molecule sonolyzed at 308 kHz

Bubble diameter ( $\mu\text{m}$ )	Bubble volume (L)	Void fraction per cycle <sup>a</sup>	Number of bubble $N$ in 1 L per cycle	Duration of one ultrasonic cycle at 308 kHz ( $\mu\text{s}$ )	Number of bubble in 1 L in 15 min <sup>b</sup>	CO <sub>2</sub> molecule number/bubble average value from (c) and (d) $f$	Predicted CO <sub>2</sub> molecule number which can be sonolyzed in 1 L average value from (c) and (d) $g = e \cdot f$
	$a$	$b$	$c = 3 \cdot b/a$	$d = 1/308000$	$e = c \cdot 15.60/d$		
62	$9.98 \times 10^{-10}$	$7.5 \times 10^{-3}$	$2.3 \times 10^7$	3.3	$6.2 \times 10^{15}$	$2.2 \times 10^{11}$	$1.4 \times 10^{27}$

<sup>a</sup> Per cycle, in the lack of precision on the final unit of data.

<sup>b</sup> Duration of the ultrasonic irradiation in Henglein experimental conditions.

<sup>c</sup> CO<sub>2</sub> molecule number calculated by means of the Henry's law constant.

<sup>d</sup> CO<sub>2</sub> molecule number calculated by means of the Van der Waals equation.

some bubbles did not lead to sonochemical reactions, or both.

In this work, the calculated number of cavitation bubble can be considered as maximum values since it has been considered that all bubbles have the same size. On the other way, it has been shown that there is an inhomogeneous bubbles distribution in size and shape generated in the medium under the pressure field [34,37]. It is also known that large bubbles aggregate and degas out from the bulk and do not collapse [34,38,39]. Then two kind of cavitation bubbles can be considered: the fragmentary transient cavitation bubble who collapse in one acoustic cycle and the repetitive transient cavitation bubbles who does not collapse, and which life time is several acoustic cycles [9,40]. So in the simple model presented in this work, the number of bubbles and the amount of collapsing bubbles seems to be overestimated.

According to the sonolysis of CO<sub>2</sub>, it is then possible to give a percentage of efficient bubbles which correspond to the yield of the experimental CO molecule number formed to the theoretical CO expected, i.e.  $7.21 \times 10^{20} / 1.4 \times 10^{27} = 5.2 \times 10^{-7}$ . That means that either one molecule on 1900000 is sonolyzed or that one bubble on about 1900000 is an efficient bubble leading to the sonolysis of CO<sub>2</sub>. This result is closely dependant from the void fraction used and not so much from the bubble size hypothesis. The final result is also in a good agreement with experimental observations at high frequency since usually for a 1 mM solution of organic compound, a total degradation is got after about 1 h [41]. Indeed, investigations in the present paper lead to a bubble number of  $24.8 \times 10^{15}$  for 1 L and in 1 h. As about 1 bubble on 1900000 is an efficient bubble, that means that  $1.3 \times 10^{10}$  bubbles are finally efficient for leading sonochemistry. On the other hand, as  $4.5 \times 10^{10}$  molecules can be present within the bubble, it is  $1.3 \times 10^{10} \times 4.5 \times 10^{10} = 5.9 \times 10^{20}$  molecules which can be degraded, in a very good agreement with the initial 1 mM degraded for 1 L and in 1 h, i.e.:  $1 \times 10^{-3} \times 6.02 \times 10^{23} = 6 \times 10^{20}$  molecules.

It is then quite difficult to conclude to a gas pumping effect by cavitation bubbles. Based on this work, it can be only concluded that the CO<sub>2</sub> concentration do not exceed the Henry law predictions. The variation in the shape and dimension of the cavitation bubbles until their collapse does not exclude a temporal pumping of the dissolved CO<sub>2</sub> inside the bubbles.

## 5. Concluding remarks

It has been shown that the statistical thermodynamic can be an useful tools for the thermodynamic characterization of the ultrasonic reactions by the calculation of the most favorable temperature and pressure. It also allows to predict the thermodynamic area where the reaction is favored within the bubble of cavitation. The decomposition of CO<sub>2</sub> is then favored in the first shell of the cavitation bubble whereas the decomposition of O<sub>2</sub> is

thermodynamically favored in the very hot heart of the bubble instead of its formation. Nevertheless, O<sub>2</sub> is kinetically formed as it has been experimentally quantified by Henglein. This fact points out the need to couple together the thermodynamic and the kinetic data. The recombination of H and O atoms into H<sub>2</sub>O is thermodynamically favored at ambient pressure and temperature at the bubble/bulk interface.

To the contrary of an expected pumping effect of dissolved CO<sub>2</sub> in the liquid, within the bubble of cavitation, it has been observed that the calculated number of cavitation bubble is enough higher to get the experimentally CO amount formed by the sonolysis of CO<sub>2</sub>. The difference between experimental and theoretical CO amount leads to predict that only one bubble on about 1900000 is sonochemically active at 300 kHz.

## Acknowledgements

Authors thank Martin Bilodeau from the Faculté des Arts et des Sciences – Mathématiques et Statistique, at Montreal University and referee for very constructive discussions.

## ANNEX 1

The partition function  $Z$  from the in thermodynamic statistic uses energy term of the system in a particular state which can in principle be calculated independently or by using the most advanced *ab initio* techniques. In this last field appear the Hartree–Fock (HF) method, the Semi-empirical method, the Density Functional Theory (DFT) or the Bond-Additivity Corrections (BAC) method, which can be applied with different level of approximation such as the fourth-order Moller–Plesset (MP4) perturbation theory or G2 level (an example of coupling theory with theory, in contrast to coupling theory with experiment [42] – see Sandia Natl. Lab. at <http://herzberg.ca.sandia.gov>).

Using *ab initio* calculations allows in part to determine thermodynamic properties of reactants, intermediate radicals, and transition state structures especially toward combustion and gas phase modelling. As example, enthalpies of formation ( $\Delta H_{f,298}^\circ$ ) can be determined using the Complete Basis Set (CBSQ) composite method and by DFT calculations. Properties such as entropies ( $S_{298}^\circ$ ) and heat capacities  $C_p^\circ(T)$  can be determined using geometric parameters and vibrational frequencies obtained at the HF theory and also include contributions from internal rotations. Nevertheless, these data are obtained in a temperature interval ranging from 300 to 1500 K and sometimes up to 3000 K by using thermodynamic data from Chemkin or CANTERA as example. In another way, *ab initio* techniques, produce detailed molecular information by using thermodynamic information. Further calculations are needed to generate familiar quantities such as  $S^\circ$ ,  $C_p^\circ$  or  $\Delta H_f^\circ$  and scarcely thermodynamical equilibrium constant. In addition, with *ab initio*, the raw results on electronic calculations of molecular

Table 4  
Comparison between CANTERA database and statistical thermodynamic on the calculation of equilibrium constants versus T and P

Reaction	T (K)	K (CANTERA)		K (stat.thermo.)	
		at 1 bar	at 300 bar	at 1 bar	at 300 bar
(1) Ar + CO <sub>2</sub> → Ar + CO + O	10000 <sup>b</sup>	2.6 × 10 <sup>5</sup>	6 × 10 <sup>5</sup>	787	1914
	3300 <sup>a</sup>	0.079	632	2.2 × 10 <sup>-4</sup>	2.2
	300 <sup>a</sup>	1.9 × 10 <sup>-86</sup>	5.9 × 10 <sup>-44</sup>	6.7 × 10 <sup>-89</sup>	6.9 × 10 <sup>-46</sup>
(2) Ar + O <sub>2</sub> → Ar + O + O	10000 <sup>b</sup>	6 × 10 <sup>4</sup>	5.6 × 10 <sup>5</sup>	200	1874
	3300 <sup>a</sup>	0.02	636	5.7 × 10 <sup>-5</sup>	2.3
	300 <sup>a</sup>	4.9 × 10 <sup>-82</sup>	8.7 × 10 <sup>-44</sup>	1.6 × 10 <sup>-84</sup>	4.5 × 10 <sup>-46</sup>
(3) Ar + 2H + O → Ar + H <sub>2</sub> O	10000 <sup>b</sup>	3.8 × 10 <sup>-5</sup>	8.4 × 10 <sup>-10</sup>	3.6	8.2 × 10 <sup>-5</sup>
	3300 <sup>a</sup>	2.5 × 10 <sup>5</sup>	2.8 × 10 <sup>-6</sup>	2.8 × 10 <sup>10</sup>	2.3 × 10 <sup>-3</sup>
	300 <sup>a</sup>	1 × 10 <sup>154</sup>	9 × 10 <sup>42</sup>	9 × 10 <sup>158</sup>	1 × 10 <sup>41</sup>

<sup>a</sup> Compute with Mixmaster.

<sup>b</sup> With the help of tutorials from Python GUI application, because of Mixmaster limitations.

Table 5  
The main characteristics on available databases used in the combustion field

Database	Characteristics	Maximum temperature used
CANTERA	• Used for problems involving chemically-reacting flows. Thermodynamic data (equilibrium constant) and kinetics data are available with Mixmaster	3500 K
	• Python-GUI application allows to get higher temperature limit	10000 K
GRI-Mech	A list of elementary chemical reactions and associated rate constant expressions. Good representation of natural gas flames and ignition, and can be used especially for studying a multiphase chemical equilibrium	3000 K
Chemkin	Determination of the most important initial reaction pathways of reactions, with an estimation of rate constants (using Quantum Rice-Ramsperger-Kassel (QRRK) analysis) arising from thermodynamic data	2000 K
Sandia	Thermodynamic data are direct result of the BAC calculation and can fit with Chemkin	4000 K

energy, do not correspond to properties at absolute zero temperature and must always be corrected [43,44] (see NIST Lab. at <http://srdata.nist.gov/cccbdb/thermo.asp>). All the corrections are based upon molecular spectroscopy, with temperature-dependence implicit in the molecular partition function. The partition function is then used not only for theoretical predictions with the previous techniques, but also to generate most published thermochemical tables. Calculations by means of statistical thermodynamics appear then as one way to compute properties as functions of temperature and pressure. Nevertheless, assumptions on some data (mainly the spectroscopic data) must be done especially at very high *T* and *P*, since these extreme conditions can be still considered as an unknown field.

It must be mentioned that the calculation of the full partition function of complex chemical reaction from *ab initio* is not presently feasible. However, well-established controllable approximations (Born-Oppenheimer) and methods exist to split the partition function into relevant contributions which can be handled by *ab initio* techniques.

As comparison is often done between what it is happened in a cavitation bubble and combustion reactions [45–47], it is also of interest to consider thermodynamic databases in combustion. Nevertheless, these databases have limitations especially at high temperature (Table 5). In addition, as seen above, the association of statistical

thermodynamic with *ab initio* calculations is sometimes required. So in the same way that databases available in the field of combustion studies, statistical thermodynamic can also be considered as a useful tools for the prediction of thermodynamic data especially for temperature higher than 3000 K.

One conclusion which can be underlined is on the utility of any of these methods to chemists who are seeking missing data. The choice will depend on the nature of the compound in which they are interested, the accuracy of the method, the chemists experience in computational chemistry and of course the computing equipment available to them.

## ANNEX 2

It is interesting to compare values of the three equilibrium constants obtained by the statistical thermodynamic with classical thermodynamic database from Python 2.4.2 version (<http://www.cantera.org>, CANTERA soft from D. Goodwin, Mixmaster application). The soft is on a free-access and can be downloaded quite easily. It allows to get kinetic and equilibrium constants on reactions occurring especially at high temperature. Calculations about the three equilibrium constants carried out under an Argon

atmosphere and some characteristic data are reported in Table 4.

The main conclusion is that evolutions are the same in both cases, but an important discrepancy on the absolute values  $K$  is observed especially at low temperature where  $K$  focuses on  $\pm$ infinity. However, a quite good accordance is got at high temperature for reaction (1) and (2). It can be noticed that this paper has no pretension concerning the determination of absolute values of  $K$ .

### ANNEX 3

Computation of the bubble radius at 300 kHz has been performed according to the following Rayleigh–Plesset equation [9]:

$$f = \frac{1}{R_0 \sqrt{\rho}} \cdot \sqrt{3\kappa \cdot \left( P_{hyd.} + \frac{2\sigma_w}{R_0} - P_v \right) - \frac{2\sigma_w}{R_0} + P_v - \frac{4\eta^2}{\rho \cdot R_0^2}} \quad (10)$$

This simple equation allows to get  $R_0$ , the unknown equilibrium radius value, which is considered as the greatest limit value for bubble radius which undergo unstable or transient cavitation leading to the collapse of bubbles. Consequently, above this limit value, bubbles are stable bubbles and are associated to the small-amplitude approximation.

### References

- [1] K.S. Suslick, *Science* 247 (1990) 1439.
- [2] W.B. McNamara III, Y.T. Didenko, K.S. Suslick, *Nature* 401 (1999) 772.
- [3] D.J. Flannigan, K.S. Suslick, *Nature* 434 (2005) 52.
- [4] K. Yasui, T. Tuziuti, M. Sivakumar, Y. Iida, *J. Chem. Phys.* 122 (2005) 224706–224711.
- [5] A.J. Colussi, L.K. Weavers, M.R. Hoffmann, *J. Phys. Chem. A* 102 (1998) 6927.
- [6] J. Rae, M. Ashokkumar, O. Eulaerts, C. Von Sonntag, J. Reisse, F. Grieser, *Ultrason. Sonochem.* 12 (2005) 325.
- [7] E. Ciawi, J. Rae, M. Ashokkumar, F. Grieser, *J. Phys. Chem. B* 110 (2006) 13656.
- [8] W.B. McNamara III, Y.T. Didenko, K.S. Suslick, *J. Phys. Chem. B* 107 (2003) 7303.
- [9] T.G. Leighton, in: *The Acoustic Bubble*, Academic Press, London, 1994.
- [10] S. Dähnke, K.M. Swamy, F.J. Keil, *Ultrason. Sonochem.* 6 (1999) 31.
- [11] T. Lepoint, F. Lepoint-Mullie, in: J.-L. Luche (Ed.), *Synthetic Organic Sonochemistry*, Plenum Press, NY, 1998, p. 1.
- [12] C. Pétrier, Y. Jiang, M.-F. Lamy, *Environ. Sci. Technol.* 32 (18) (1998) 1316.
- [13] B. David, M. Lhote, V. Faure, P. Boule, *Water Res.* 32 (8) (1998) 2451.
- [14] B. David, D. Riguier, *Ultrason. Sonochem.* 9 (2002) 45.
- [15] L.K. Weavers, F.H. Ling, M.R. Hoffmann, *Environ. Sci. Technol.* 32 (18) (1998) 2727.
- [16] A. Henglein, *Z. Naturforsch.* 40b (1984) 100.
- [17] J. Wanartz, U. Maas, R.W. Dibble, *Chemical kinetics*, in: *Combustion, Physical and Chemical Fundamentals, Modelling and Simulation, Experiments, Pollutant Formation*, Springer, 1995, p. 63.
- [18] A.J. Szeri, B.D. Storey, A. Pearson, J.R. Blake, *Phys. Fluids* 15 (9) (2003) 2576.
- [19] B.E. Noltingk, E. Neppiras, *Proc. Phys. Soc. B* 63 (1950) 674.
- [20] M.E. Fitzgerald, V. Griffing, J. Sullivan, *J. Chem. Phys.* 25 (5) (1956) 926.
- [21] G. Emschwiller, in: *Chimie Physique - Tome I*, Presses Universitaires de France, 1959, p. 343.
- [22] C. Chahine, P. Devaux, in: *Thermodynamique Statistique*, Dunod, Paris, 1976, p. 102.
- [23] O. Dessaux, P. Goudmand, F. Langrand, in: *Thermodynamique Statistique Chimique*, Dunod, 1982, p. 32.
- [24] I.N. Herstein, in: *Fields: Solvability by Radicals in Topics in Algebra*, J. Wiley & Sons, Inc., 1975, p. 250.
- [25] I. Barin, in: *Thermochemical Data of Pure Substances – Part I*, VCH, 1993, p. 271.
- [26] P.W. Atkins, J. De Paula, in: *Chimie Physique*, seventh ed., De Boeck University, 2004, p. 145.
- [27] M.P. Brenner, S. Hilgenfeldt, D. Lohse, *Rev. Mod. Phys.* 74 (2002) 425.
- [28] M. Minnaert, *Phil. Mag.* 16 (1933) 235.
- [29] G. Cum, G. Galli, R. Gallo, A. Spadaro, *Ultrasonics* 30 (1992) 267.
- [30] C.M. Sehgal, S.Y. Wang, *J. Am. Chem. Soc.* 103 (1981) 6606.
- [31] H. Lin, B.D. Storey, A.J. Szeri, *J. Fluid Mech.* 452 (2002) 145.
- [32] W.C. Moss, J.L. Levatin, A.J. Szeri, *Proc. R. Soc. A: Math. Phys. Eng. Sci.* 4556 (2000) 2983.
- [33] V. Ragaini, C.L. Bianchi, in: J.-L. Luche (Ed.), *Synthetic Organic Sonochemistry*, Plenum Press, NY, 1998, p. 235.
- [34] F. Burdin, N.A. Tsochatzidis, P. Guiraud, A.-M. Wilhelm, H. Delmas, *Ultrason. Sonochem.* 6 (1999) 43.
- [35] S. Labouret, PhD thesis, University of Valenciennes, France, 1998.
- [36] S. Labouret, I. Looten-Baquet, J. Frohly, F. Haïne, *Ultrasonics* 36 (1998) 603.
- [37] T.G. Leighton, *Ultrason. Sonochem.* 2 (2) (1995) S123.
- [38] S. Luther, R. Mettin, P. Koch, W. Lauterborn, *Ultrason. Sonochem.* 8 (2001) 159.
- [39] R. Mettin, S. Luther, W. Lauterborn, in: *Proceedings of the 2nd Conference on Applications of Power Ultrasound in Physical and Chemical Processing, PROGEP, Toulouse – France, 6–7 May (1999)* 125.
- [40] G. Servant, J.L. Laborde, A. Hita, J.P. Caltagirone, A. Gérard, *Ultrason. Sonochem.* 10 (6) (2003) 347.
- [41] C. Pétrier, A. Francony, *Ultrason. Sonochem.* 4 (1997) 295.
- [42] C. Melius, in: *Symposium on Computational Thermochemistry Computers in Chemistry Division of the American Chemical Society, 21th National Meeting, Orlando, Florida, August 25–29 (1996)*.
- [43] A.P. Scott, L. Radom, *J. Phys. Chem.* 100 (1996) 16502.
- [44] K.K. Irikura, D.J. Frurip, in: *Computational Thermochemistry: Prediction and Estimation of Molecular Thermodynamics*, American Chemical Society, 1998.
- [45] A. Henglein, *Ultrasonics* 25 (1) (1987) 6.
- [46] E.J. Hart, C.-H. Fischer, A. Henglein, *Int. J. Radiat. Appl. Instr. Part C., Radiat. Phys. Chem.* 36 (4) (1990) 511.
- [47] C. Pétrier, E. Combet, T. Mason, *Ultrason. Sonochem.* 14 (2007) 117.